Bromine-81 Nuclear Quadrupole Resonance and Aluminum-27 Nuclear Magnetic Resonance in $AlBr_3$ Complexes

Tsutomu OKUDA, Hideta ISHIHARA, Koji YAMADA, and Hisao NEGITA

Department of Chemistry, Faculty of Science, Hiroshima University, Hiroshima 730

(Received July 7, 1977)

The Zeeman effect on ^{81}Br NQR and the quadrupole effect on ^{27}Al NMR in L·$AlBr_3$ complexes (L=KBr, $POBr_3$, and H_2S) were studied at room temperature. It was found that the ^{27}Al quadrupole-coupling constant for these complexes decreases with decreasing coupling constant of the ^{81}Br atom in –$AlBr_3$ and that the atomic arrangement about the Al atom has C_{3v} symmetry in $POBr_3$·$AlBr_3$ and H_2S·$AlBr_3$. In the latter complex, H_2S molecule is reorientated at room temperature. The amount of charge transfer in these complexes was estimated on the basis of the Townes-Dailey theory and the bond angle ∠Br–Al–Br was found to depend on the amount of the charge transfer. The temperature dependence of the ^{81}Br NQR frequencies was observed in order to obtain information about molecular motion in H_2S·$AlBr_3$ and $POBr_3$·$AlBr_3$.

For L·$AlBr_3$ molecular complexes (L=ligand), the charge distribution of the acceptor molecule can be determined on the basis of the Townes-Dailey theory which is relatively simple but appears to still be valuable.[1,2] In order to estimate the charge distribution using this procedure, it is necessary to determine the ∠Br–Al–Br bond angles and the quadrupole-coupling constants for both Al and Br atoms. Some research employing NQR has already been reported on L·$AlBr_3$ molecular complexes.[3–5] All, however, was performed on polycrystalline samples. Therefore, an attempt was made to observe the Zeeman effect on ^{81}Br NQR and the quadrupole effect on ^{27}Al NMR using single crystals.

Experimental

KBr·$AlBr_3$ and $POBr_3$·$AlBr_3$ were prepared by mixing equimolar amounts of the relevant compounds. H_2S·$AlBr_3$ was prepared by passing hydrogen sulfide through a carbon disulfide solution of aluminum bromide.[6] The single crystals were grown employing the Bridgman-Stockbarger method. The melting points of these complexes are as follows: 191 °C for KBr·$AlBr_3$, 181 °C for $POBr_3$·$AlBr_3$, and 83 °C for H_2S·$AlBr_3$. The bromine content was determined using the Fajans method. Found: Br, 83.6%. Calcd for KBr·$AlBr_3$: Br, 82.9%. Found: Br, 87.5%. Calcd for $POBr_3$·$AlBr_3$: Br, 86.6%. Found: Br, 78.5%. Calcd for H_2S·$AlBr_3$: Br, 79.7%.

The NQR spectrometer was a self-quenching super-regenerative oscillator with frequency modulation and the resonance lines were displayed on an oscilloscope. The Zeeman effect on ^{81}Br NQR was studied using the zero-splitting cone method. A magnetic field of *ca.* 250 G was applied by means of a Helmholtz coil. ^{81}Br NQR frequencies were observed at various temperatures which were attained in a Dewar vessel by cooling petroleum ether with liquid nitrogen or heating liquid paraffin with an electric heater.

^{27}Al NMR was observed using a broad-line NMR spectrometer (Model JES-ME 1) from the Japan Electron Optics Lab. Co., Ltd. The resonance frequency was fixed at 13.00 MHz and the magnetic field was varied to obtain the resonance.

Results and Discussion

^{81}Br NQR. The NQR frequencies of ^{81}Br atoms at room temperature are listed in Table 1. For H_2S·$AlBr_3$, only one ^{81}Br NQR line was observed. This is consistent with the results of X-ray analysis,[6] that is, the bromine atoms of the complex are situated at equivalent positions in the crystal. For $POBr_3$·$AlBr_3$, two ^{81}Br NQR lines were observed. Although its crystal structure is not known at present, the formation of the O–Al bond is obvious from infrared spectroscopic studies.[7] Therefore, the structure of the complex is assumed to be Br_3P–O–$AlBr_3$. Consequently, the lower and higher resonance lines can be assigned to the Br atoms linked to the Al and P atoms, respectively, referring to the ^{81}Br NQR frequencies of Al_2Br_6 and $POBr_3$ in their pure states.[8,9] For KBr·$AlBr_3$, four ^{81}Br NQR lines were observed. The average frequency was in the same range as those of $LiAlBr_4$ and $NaAlBr_4$ and was considerably lower than that of the terminal ^{81}Br atoms of KAl_2Br_7.[10] One of the constituents of the complex was assumed to be a distorted tetrahedral ion, $AlBr_4^-$.

Table 1. NQR PARAMETERS FOR ^{81}Br AT ROOM TEMPERATURE

Compound		Frequency (MHz)	η (%)	$e^2Qq_{zz}h^{-1}$ (MHz)
H_2S·$AlBr_3$		81.69	8.1±0.8	163.20
$POBr_3$·$AlBr_3$	ν_a	78.70	1.9±0.7	157.39
	ν_b	211.07	2.6±0.6	422.09
KBr·$AlBr_3$	ν_a	76.31	3.1±0.3	152.60
	ν_b	77.56	24.4±0.7	153.60
	ν_c	78.27	10.8±0.7	156.23
	ν_d	79.91	7.5±0.7	159.66

The zero-splitting patterns were obtained from the Zeeman effect at room temperature and are shown in Figs. 1—3. The bond angles ∠Br–M–Br (M=Al and P) can be deduced, if the principal z axis of the ^{81}Br EFG tensor is assumed to be parallel to the direction of the M–Br bond. The results thus obtained are listed in Table 2.

For H_2S·$AlBr_3$, X-ray analysis of the powder sample shows that there is only one type of $AlBr_3$ unit in the crystal, and three zero-splitting patterns are expected.[6] However, six zero-splitting patterns were obtained, as is shown in Fig. 1. Accordingly, it is evident that there are two kinds of $AlBr_3$ units which differ only in the orientation in the crystal. More precise X-ray analysis is necessary in order to clarify the crystal structure of this complex.

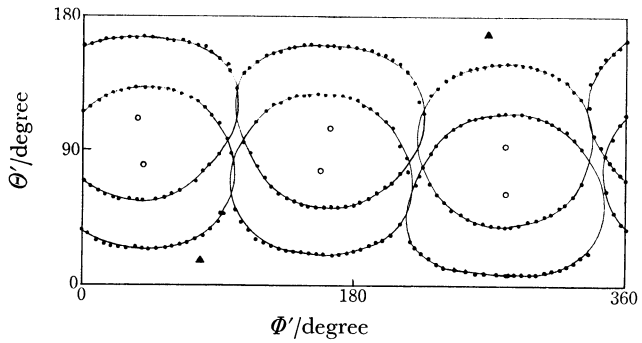

Fig. 1. Zero-splitting patterns of ^{81}Br Zeeman lines in $H_2S \cdot AlBr_3$. The direction of the three-fold axis is indicated by ▲. Θ' and Φ' are polar and azimuthal angles, respectively, in the coordinate fixed to the sample.

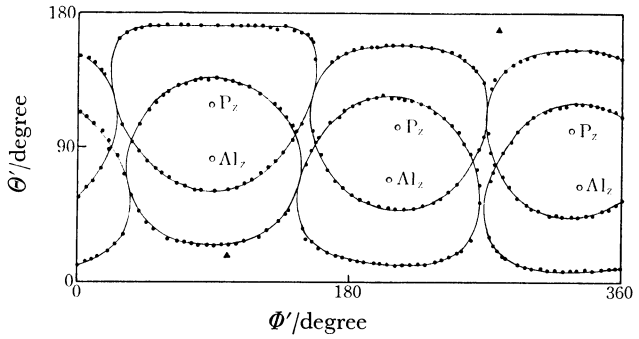

Fig. 2. Zero-splitting patterns of ^{81}Br Zeeman lines in $POBr_3 \cdot AlBr$. The direction of the principal z axes of the EFG tensors at the ^{81}Br atoms linked to the Al and P atom are indicated by Al_z and P_z, respectively. The direction of the three-fold axis is indicated by ▲. Θ' and Φ' are polar and azimuthal angles, respectively, in the coordinate fixed to the sample.

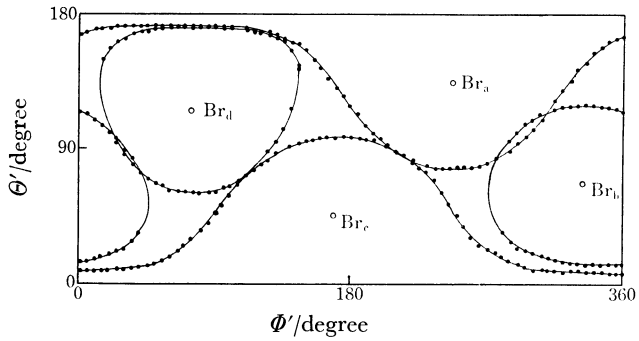

Fig. 3. Zero-splitting patterns of ^{81}Br Zeeman lines in $KBr \cdot AlBr_3$. The subscripts correspond to those of the resonance lines. Θ' and Φ' are polar and azimuthal angles, respectively, in the coordinate fixed to the sample.

For $POBr_3 \cdot AlBr_3$, the three-fold axis is found to be parallel to the P–O–Al bond which has a bond angle of 180.0±0.7°, because the three-fold axis of $AlBr_3$ is parallel to that of $POBr_3$ to within 0.7° from the result of the Zeeman effect. The configuration of $AlBr_3$ relative to $POBr_3$ is eclipsed, as is shown in Fig. 2. In $KBr \cdot AlBr_3$, the atomic arrangement about the Al atom is approximately tetrahedral, as is shown in Table 2, and the average bond angle is 109.5°.

Table 2. Bond angles ∠Br-M-Br

Compound	M	∠Br-M-Br (degree)	
$H_2S \cdot AlBr_3$	Al	112.7±0.4	
$POBr_3 \cdot AlBr_3$	Al	111.8±0.7	
	P	109.4±0.5	
$KBr \cdot AlBr_3$[a)]	Al	105.8±0.4	108.2±0.3
		109.4±0.5	110.1±0.3
		111.7±0.3	111.8±0.1

a) Six bond angles can be determined because four bromine atoms are nonequivalent.

The value of the asymmetry parameter, η, was determined using the following equation,[11)]

$$\sin^2\Theta = 2/(3-\eta\cos 2\Phi), \quad (1)$$

where Θ and Φ are the polar and azimuthal angles of the Zeeman magnetic field with respect to the principal coordinates of the EFG tensor at the resonating nucleus. Consequently, the quadrupole-coupling constant, e^2Qq_{zz}/h, of the ^{81}Br atom was calculated using

$$\nu = (e^2Qq_{zz}/2h)(1+\eta^2/3)^{1/2}, \quad (2)$$

where ν is the ^{81}Br NQR frequency. The value of η and e^2Qq_{zz}/h thus obtained are listed in Table 1.

^{27}Al NMR. Only one central resonance line ($m=+1/2 \leftrightarrow m=-1/2$), which was affected by the second-order quadrupole interaction, was observed for both $H_2S \cdot AlBr_3$ and $POBr_3 \cdot AlBr_3$. The rotation patterns of the central line were obtained by measuring the shift, ΔH, from the magnetic field H_L corresponding to a Larmor frequency ν_L of 13.00 MHz, when the sample was rotated about the rotation axis perpendicular to the external magnetic field. The results are shown in Fig. 4. The frequency shift, $\Delta\nu$, can be represented in terms of the magnetic field by the following equation:[12)]

$$\Delta\nu = -\nu_L(\Delta H/H_L^2)(\Delta H+H_L). \quad (3)$$

Since the components >S–$AlBr_3$ in $H_2S \cdot AlBr_3$ and –O–$AlBr_3$ in $POBr_3 \cdot AlBr_3$ have C_{3v} symmetry, respectively, the frequency shift of the central line was analyzed using the following equation derived from second-order perturbation theory with $\eta=0$,[13)]

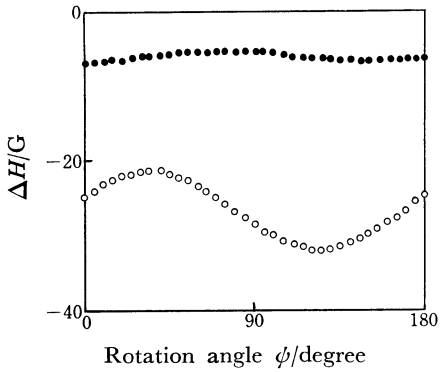

Fig. 4. Rotation patterns of ^{27}Al NMR central lines. $H_2S \cdot AlBr_3$ (○) for $\delta=10.5°$ and $\phi_o=35.0°$. $POBr_3 \cdot AlBr_3$ (●) for $\delta=8.5°$ and $\phi_o=70.0°$.

$$\Delta\nu = -(\nu_Q^2/16\nu_L)(a-3/4)(1-\mu^2)(9\mu^2-1), \quad (4)$$

where $\nu_Q=3e^2Qq/2I(2I-1)h$, $a=I(I+1)$, and $\mu=\sin\delta\cos(\psi-\psi_0)$. δ is the angle between the rotation axis and the principal z axis of the ^{27}Al EFG tensor. ψ is the rotation angle and ψ_0 is the value when the principal z axis lies in the plane formed by the rotation axis and the magnetic field.

Neither first- nor second-order splitting of ^{27}Al NMR spectra in $KBr\cdot AlBr_3$ were observed, so that the ^{27}Al quadrupole-coupling constant is estimated to be less than 1.3 MHz from the line width of the spectrum in the polycrystalline sample.

The ^{27}Al quadrupole-coupling constants thus obtained are as follows: 9.1±0.1 MHz for $H_2S\cdot AlBr_3$, 4.2±0.1 MHz for $POBr_3\cdot AlBr_3$, and less than 1.3 MHz for $KBr\cdot AlBr_3$. It was found that the ^{27}Al quadrupole-coupling constants for these complexes decrease with decreasing coupling-constant of the ^{81}Br atom in the $-AlBr_3$ components. A similar relation has been obtained by Tong[14] between the NQR frequencies of ^{69}Ga and ^{35}Cl atoms in L–$GaCl_3$ molecular complexes (L=ligand).

The Bond Character. The amount of charge transfer in these molecular complexes were estimated according to the Townes-Dailey theory. Supposing C_{3v} symmetry for hybrid orbitals centered at the Al atom, the four orthonormal hybrid wavefunctions can be expressed by[2]

$$\begin{aligned}\psi_1 &= s_1\phi_s + (1-s_1^2)^{1/2}\phi_{p_z},\\ \psi_2 &= s_2\phi_s + (1-s_2^2)^{1/2}\{\phi_{p_z}\cos\theta-\phi_{p_x}\sin\theta\},\\ \psi_3 &= s_2\phi_s + (1-s_2^2)^{1/2}\{\phi_{p_z}\cos\theta+(1/2)\phi_{p_x}\sin\theta\\ &\qquad -(\sqrt{3}/2)\phi_{p_y}\sin\theta\},\end{aligned} \quad (5)$$

and

$$\psi_4 = s_2\phi_s + (1-s_2^2)^{1/2}\{\phi_{p_z}\cos\theta+(1/2)\phi_{p_x}\sin\theta + (\sqrt{3}/2)\phi_{p_y}\sin\theta\},$$

where θ is the angle ∠Br–Al–L (L=ligand). s_1^2 and s_2^2 represent the fractional s character of the Al–L and Al–Br bonds, respectively. The population of orbital ψ_1, which is directed toward the ligand, is denoted by a_{Al} and the population of orbitals ψ_2, ψ_3, and ψ_4, which are directed toward the Br atoms, by b_{Al}. Then, the total electric field gradient of the Al atom is given by

$$q_{zz}(^{27}Al) = (b_{Al}-a_{Al})\{3-2/\sin^2\theta\}q_{at}. \quad (6)$$

It is evident that from the spherical triangle that there exists a relation such that $\cos^2\theta=(2\cos\alpha+1)/3$, where α is the ∠Br–Al–Br angle. Considering the increase in the EFG due to positive ionization of the Al atom, the quadrupole-coupling constant is given by

$$e^2Qq_{zz}/h(^{27}Al) = (b_{Al}-a_{Al})\{-3\cos\alpha/(1-\cos\alpha)\} \times (1+\varepsilon_{Al}\rho_{Al})e^2Qq_{at}/h(^{27}Al). \quad (7)$$

On the other hand, the ^{81}Br quadrupole-coupling constant is given by[2]

$$e^2Qq_{zz}/h(^{81}Br) = \{(1-s^2)(2-b_{Br})/(1+\varepsilon_{Br}\rho_{Br})\} \times e^2Qq_{at}/h(^{81}Br), \quad (8)$$

where s^2 is the fractional s character of the Br–Al σ orbital and b_{Br} is the population of this orbital. In Eqs. 7 and 8, $e^2Qq_{at}/h(^{27}Al)$ and $e^2Qq_{at}/h(^{81}Br)$ are the atomic quadrupole-coupling constants, the ε are parameters which correct for the ionization, and ρ_{Al} and ρ_{Br} are the positive and negative charges, respectively. The ρ are related to the population numbers by $\rho_{Al}=3-(3b_{Al}+a_{Al})$ and $\rho_{Br}=b_{Br}-1$. It is assumed that $b_{Al}+b_{Br}=2$ and $b_{Al}>a_{Al}$. Furthermore, s and ε the were chosen such that $s^2=0.15$, $\varepsilon_{Br}=0.13$, and $\varepsilon_{Al}=0.27$.[15]

Table 3. Population numbers a_{Al}, b_{Al}, and b_{Br}

Compound	a_{Al}	b_{Al}	b_{Br}
$H_2S\cdot AlBr_3$	0.13	0.33	1.67
$POBr_3\cdot AlBr_3$	0.22	0.31	1.69
$KBr\cdot AlBr_3$	0.30	0.30	1.70
	0.31	0.31	1.69
	0.31	0.31	1.69
	0.32	0.32	1.68

The values of a_{Al}, b_{Al}, and b_{Br} can be calculated from Eqs. 7 and 8, using the values of the bond angles and the quadrupole-coupling constants. The results are listed in Table 3. For $KBr\cdot AlBr_3$, a_{Al} is assumed to be equal to b_{Al}, because it cannot be specifield which bromine atom participate in the coordinate ion. Then it is evident that the donor powers of the ligands increase in the order $H_2S<POBr_3<Br^-$, provided that a_{Al} is regarded as a measure of the amount of charge transfer. In this connection, both ^{81}Br and ^{27}Al quadrupole-coupling constants in $-AlBr_3$ decrease with increasing a_{Al} or increasing degrees of charge transfer. In addition, it is seen that the bond angle approaches the tetrahedral angle with increasing a_{Al}. Therefore, in consideration of the results of the molecular-orbital calculation shown below, it appears that as the $AlBr_3$ in the complex approaches the tetrahedral arrangement, the strength of the donor-acceptor bond increases.

For BCl_3 and BF_3, the effect of reorganization has been explained using the results of CNDO/2 molecular-orbital calculations.[16] In the present investigation, an extended Hückel method for $AlBr_3$ was carried out.[17] The calculated lowest unoccupied virtual-orbital energy, E(LUMO), and the total electronic energy, E(ELEC), are presented as a function of the bond angle ∠Br–Al–Br in Fig. 5. This figure shows that E(LUMO) decreases with the reorganization of the planar molecule to the pyramidal form, in other words, the electron affinity of $AlBr_3$ increases with the reorganization, resulting in the formation of a stronger donor-acceptor bond. Meanwhile, the energy required to reorganize the planar molecule to the pyramidal form has been estimated by Cotton and Leto[18] to be 27.9 kcal/mol for $AlBr_3$, and this cannot be explained by only the change in E(ELEC) upon reorganization, as is shown in Fig. 5.

Upon the formation of a complex, the reorganization of a ligand is also considered to play an important role. According to the Zeeman effect on ^{81}Br NQR, the bond angle ∠Br–P–Br in $POBr_3\cdot AlBr_3$ is greater than that in $POBr_3$. Analogously, the H–H distance in H_2S is found from the results of the ^{1}H NMR studies to become larger upon the formation of $H_2S\cdot AlBr_3$, as is shown below. The second moment of the ^{1}H

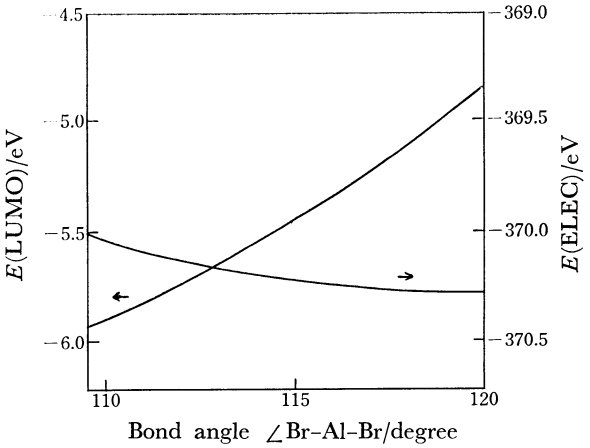

Fig. 5. Calculated energies for E(LUMO) and E(ELEC) as a function of the bond angle ∠Br-Al-Br.

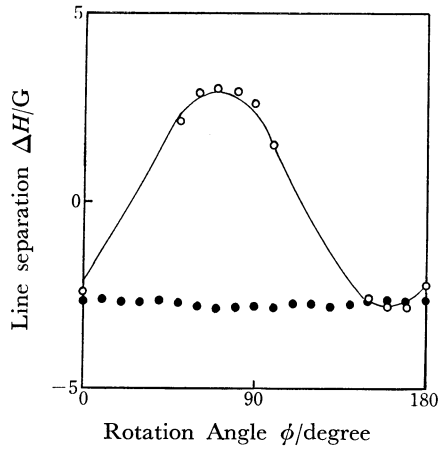

Fig. 6. Line separations in ^{1}H NMR spectra for $H_2S \cdot AlBr_3$. Sample A (○) for $\delta' = 22.8°$ and $\phi_0' = 71.4°$ Sample B (●) for $\delta' = 79.5°$ and $\phi_0' = 160.0°$.

NMR spectrum for the polycrystalline sample is 1.8—2.5 G[2] over the temperature range from 108 to 300 K and this suggests that reorientation of a proton pair takes place. The rotation patterns of the line separation of the ^{1}H NMR spectrum for two different single crystals were observed at room temperature and are shown in Fig. 6. Since the reorientation is considered to take place about the apparent three-fold axis along the S–Al bond, the line separation was analyzed according to[19]

$$\Delta H = (3/2)\mu r^{-3}\{3\cos^2\delta' \cos^2(\phi' - \phi_0') - 1\} \, | \, (3\cos^2\gamma - 1) \, | \, , \quad (9)$$

where the notations are the same with those used by Rangarajan and Ramakrishna. From this analysis, the reorientation axis was found to be consistent with the three-fold axis to within 3° and it was found that $|(3/2)\mu r^{-3}(3\cos^2\gamma - 1)| = 2.27$ G. Using this value and a Gaussian component line chosen by Pake,[20] $S(H - H_0) = \exp\{-(H - H_0)^2/2\beta^2\}$ with $\beta = 0.8$ G, the spectrum for the polycrystalline sample at room temperature can be reproduced. If the H–H line is assumed to be perpendicular to the apparent three-fold axis, the H–H distance is estimated to be 2.1 Å, which is larger than 1.88 Å from the result of NMR for H_2S in the solid phase.[21]

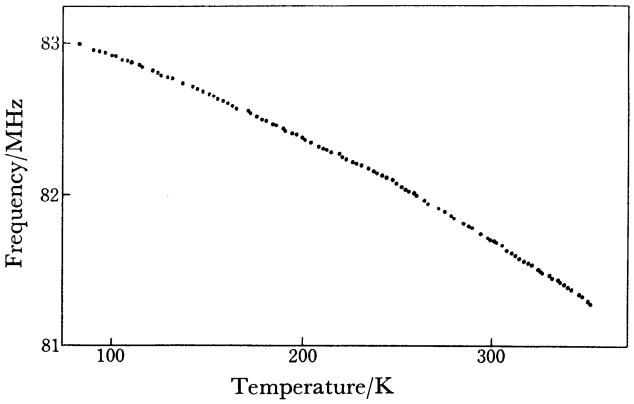

Fig. 7. Temperature dependence of ^{81}Br NQR frequency in $H_2S \cdot AlBr_3$.

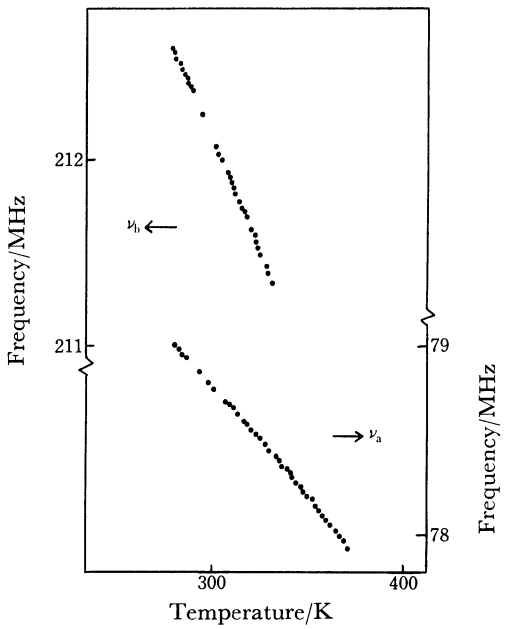

Fig. 8. Temperature depences of ^{81}Br NQR frequencies, ν_a and ν_b in $POBr \cdot AlBr_3$.

Temperature Dependence of the ^{81}Br NQR Frequencies. For $H_2S \cdot AlBr_3$, one ^{81}Br NQR line was observed at temperatures from 77 K to the melting point and the frequency decreases monotonically with increasing temperature, as is shown in Fig. 7. For $POBr_3 \cdot AlBr_3$, upon cooling, both ^{81}Br NQR lines of $AlBr_3$ and $POBr_3$ fade out around 273 K, whereas upon warming, the resonance lines of $AlBr_3$ and $POBr_3$ fade out at around 373 and 333 K, respectively, as is shown in Fig. 8. The fading out in the high temperature range may be caused by reorientation about the three-fold axis. Similar behavior has been observed for $POCl_3 \cdot GaCl_3$,[22] although the resonance lines fade out at temperatures different from those for $POBr_3 \cdot AlBr_3$. The reason for the fading out at a lower temperature, 273 K, is not apparent at the present time.

We wish to express our gratitude to Dr. Masaru

Ohsaku and Mr. Norihisa Bingo of Hiroshima University for the molecular-orbital calculations.

References

1) E. A. C. Lucken, *Fortschr. Chem. Forsh.*, **30**, 155 (1972).
2) T. Deeg and A. Weiss, *Ber. Bunsenges. Phys. Chem.*, **79**, 497 (1975).
3) L. A. Lobanova, E. N. Gur'yanova, A. F. Volkov, and R. R. Shifrina, *Zh. Obshch. Khim.*, **45**, 1857 (1975).
4) Yu. K. Maksyutin, E. V. Bryukhova, G. K. Semin, and E. N. Gur'yanova, *Izv. Akad. Nauk SSSR, Ser. Khim.*, **1968**, 2658.
5) T. Deeg and A. Weiss, *Ber. Bunsenges. Phys. Chem.*, **80**, 2 (1976).
6) A. Weiss, R. Plass, and A. Weiss, *Z. Anorg. Allg. Chem.*, **283**, 390 (1956).
7) W. Van der Veer and F. Jellinek, *Recl. Trav. Chim. Pay-Bas.*, **89**, 833 (1970). Von E. W. Wartenberg and J. Goubeau, *Z. Anorg. Allg. Chem.*, **329**, 269 (1964).
8) T. Okuda, H. Terao, O. Ege, and H. Negita, *J. Chem. Phys.*, **52**, 5489 (1970).
9) T. Okuda, K. Hosokawa, K. Yamada, Y. Furukawa, and H. Negita, *Inorg. Chem.*, **14**, 1207 (1975).
10) K. Yamada, *J. Sci. Hiroshima Univ., Ser. A*, **41**, 77 (1977).
11) C. Dean, *Phys. Rev.*, **96**, 1053 (1954).
12) M. Kasahara and I. Tatsuzaki, *J. Phys. Soc. Jpn.*, **36**, 786 (1974).
13) M. H. Cohen and F. Reif, *Solid State Physics*, **5**, 321 (1957).
14) D. A. Tong, *Chem. Commun.*, **1969**, 790.
15) B. P. Dailey and C. H. Townes, *J. Chem. Phys.*, **23**, 118 (1955).
16) D. F. Shriver and B. Swanson, *Inorg. Chem.*, **10**, 1354 (1971).
17) This calculation was carried out using the parameters which were the same as those used by Hastie and Margrave. J. W. Hastie and J. L. Margrave, *J. Phys. Chem.*, **73**, 1105 (1969). The off-diagonal terms were approximated using the equation $H_{ij}=KG_{ij}(H_{ij}+H_{ij})/2$ and $K=1.75$. Aluminum-bromine distances were fixed at 2.25 Å and calculations were carried out with sp-basis orbitals.
18) F. A. Cotton and J. R. Leto, *J. Chem. Phys.*, **30**, 993 (1959).
19) G. Rangarajan and J. Ramakrishna, *J. Chem. Phys.*, **49**, 5536 (1968).
20) G. E. Pake, *J. Chem. Phys.*, **16**, 327 (1948).
21) D. C. Look and I. J. Lowe, *J. Chem. Phys.*, **44**, 3441 (1966).
22) J. W. Jost and R. F. Schneider, *J. Phys. Chem. Solids*, **36**, 349 (1975).